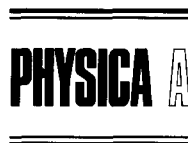




ELSEVIER

Physica A 207 (1994) 19–27



# Local porosity theory for the frequency dependent dielectric function of porous rocks and polymer blends

R. Hilfer<sup>a,b,c</sup>, B. Nøst<sup>b</sup>, E. Haslund<sup>b</sup>, Th. Kautzsch<sup>a</sup>, B. Virgin<sup>b</sup>,  
B.D. Hansen<sup>b</sup>

<sup>a</sup>*Institut für Physik, Universität Mainz, 55099 Mainz, Germany*

<sup>b</sup>*Institute of Physics, University of Oslo, P.O. Box 1048, 0316 Oslo, Norway*

<sup>c</sup>*Center for Advanced Study, Norwegian Academy of Sciences, P.O. Box 7606, 0205 Oslo, Norway*

---

## Abstract

We report preliminary results for the application of local porosity theory to dielectric response measurements on two classes of inhomogeneous systems. One class of systems are mixtures of insulators and conductors realized experimentally as sintered glass bead porous media saturated with salt water. In this case the response arises from the Maxwell–Wagner effect. The second class are mixtures of insulators realized experimentally in polymer blends where the response arises from the relaxation of atomic or molecular dipole moments. For the case of water saturated sintered glass bead systems two-dimensional local porosity distributions have been determined from digital image analysis. These measurements allow for the first time semiquantitative comparisons to previous theoretical approaches and with experiment. The dielectric measurements are used to extract the total fraction of percolating cells in the mixture. For the polymer case we show that recent concentration fluctuation models for the dielectric  $\alpha$ -relaxation arise as special cases of local porosity theory. Furthermore it is exemplified how information from static Monte-Carlo simulations of polymer blends may be useful in comparing theoretical calculations to experiment.

---

## 1. Introduction

Almost any physical system is inhomogeneous when viewed at an appropriate length scale. The theoretical problem of calculating the effective electrical properties of a mixture has a long history. The reader is referred to [15] and [14] for reviews.

Mixing laws express the effective frequency dependent dielectric function  $\epsilon_e(\omega)$  of a heterogeneous mixture in terms of the dielectric functions  $\epsilon_1(\omega)$  and  $\epsilon_2(\omega)$  of the two pure materials. Of course the “pure” materials may themselves be

heterogeneous at some smaller length scale, and in such a case  $\epsilon_1, \epsilon_2$  are themselves effective dielectric functions.

Dielectric mixing laws often employed in practice are the Clausius–Mossotti approximation [15]

$$\frac{\epsilon_e - \epsilon_1}{\epsilon_e + 2\epsilon_1} = (1 - \bar{\phi}) \frac{\epsilon_2 - \epsilon_1}{\epsilon_2 + 2\epsilon_1}, \quad (1)$$

the symmetrical effective medium theory [15]

$$\bar{\phi} \frac{\epsilon_1 - \epsilon_e}{\epsilon_1 + 2\epsilon_e} + (1 - \bar{\phi}) \frac{\epsilon_2 - \epsilon_e}{\epsilon_2 + 2\epsilon_2} = 0, \quad (2)$$

and the unsymmetrical effective medium theory [15,17]

$$\frac{\epsilon_e - \epsilon_2}{\epsilon_1 - \epsilon_2} \left( \frac{\epsilon_1}{\epsilon_e} \right)^{1/3} = \bar{\phi}. \quad (3)$$

Here  $\bar{\phi}$  denotes the volume fraction (or porosity) of component 1 defined as the volume occupied by component 1 divided by the total volume. All dielectric functions are in general complex,  $\epsilon_j(\omega) = \epsilon'_j(\omega) + i\epsilon''_j(\omega)$  ( $j = 1, 2, e$ ) and frequency dependent where  $\epsilon'_j(\omega)$ ,  $\epsilon''_j(\omega)$  denote the real and imaginary part.

Given an independent measurement of the volume fraction  $\bar{\phi}$  the mixing laws (1)–(3) can be utilized directly in comparisons with experiment. Some of us [11,16] have prepared porous media by sintering glass beads with diameters between 50  $\mu\text{m}$  and 300  $\mu\text{m}$  to different porosities between  $\bar{\phi} \approx 0.30$  and  $\bar{\phi} \approx 0.03$ . The pore space was then filled with salt water resulting in a heterogeneous mixture of glass and water. Measuring the real part  $\epsilon'_e(\omega)$  of the effective dielectric function in the frequency range between 10 kHz and 13 MHz yields a dispersion similar to the filled circles displayed in Fig. 1 [6]. The experimental results displayed in Fig. 1 have been obtained from a specimen of 250  $\mu\text{m}$  beads with  $\bar{\phi} = 0.107$  for the volume fraction of water and  $\sigma'_w(0) = 12.4 \text{ mS/m}$  for the real part of the water conductivity. The results are displayed as a function of  $\omega/\omega_w$  where  $\omega_w = \sigma'_w/\epsilon_0\epsilon'_w = 2\pi \times 2.82 \text{ MHz}$  is a characteristic water frequency,  $\epsilon'_w$  is the real part of the dielectric constant of water and  $\epsilon_0$  is the dielectric permittivity of the vacuum.

Lines of Fig. 1 represent the theoretical predictions from Eqs. (1)–(3). The dot-dashed line gives the prediction of the unsymmetrical effective medium theory Eq. (3) and the dotted line is the symmetrical effective medium theory Eq. (2). The two remaining lines are both obtained with the Clausius–Mossotti approximation (1). For the solid line water is considered as the background medium, while for the dashed line glass has been chosen as the background medium. Clearly, the traditional mixing laws (1)–(3) fail in describing the dielectric dispersion seen in the experiment.

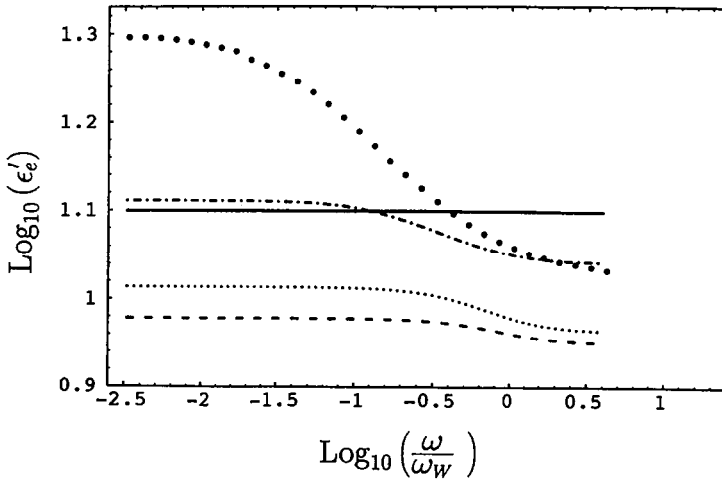


Fig. 1. Comparison of traditional mixing laws (1)–(3) with experiment. Solid circles represent the experimentally measured real part of the dielectric function for a water–glass mixture with bulk porosity (= volume fraction of water)  $\bar{\phi} = 0.107$  and water conductivity  $\sigma_w'(0) = 12.4 \text{ mS/m}$  as a function of reduced frequency  $\omega/\omega_w$  with  $\omega_w = 2\pi \times 2.82 \text{ MHz}$ . The solid line is Eq. (1) with water as the background medium, the dashed line represents Eq. (1) with glass as the background medium. The dotted line gives the prediction of Eq. (2), the dash-dotted line the prediction of Eq. (3).

## 2. Local porosity theory

As an alternative to the classical mixing laws (1)–(3) one of the authors has proposed a simple generalization of the symmetrical effective medium theory [7,8,10]. Local porosity theory replaces the characterization of the random microgeometry in terms of volume fraction or porosity  $\bar{\phi}$  by local porosity distributions  $\mu(\phi)$  and local percolation probabilities  $\lambda(\phi)$  [10]. The local porosity distribution  $\mu(\phi)$  gives the probability density to find a local porosity  $\phi$  inside a local measurement cell of linear extension  $L^*$  [7,1]. The length  $L^*$  may be calculated from the requirement of maximizing the geometric information contained in  $\mu_L(\phi)$  viewed as a function of  $L$  where  $\mu_L(\phi)$  is the local porosity distribution for measurement cells of linear extension  $L$ . Several alternative methods of determining  $L^*$  have been discussed [1]. The local percolation probability  $\lambda(\phi)$  is the fraction of percolating cells with given local porosity  $\phi$ . The generalization of the mixing law (2) may then be written as

$$\int_0^1 \frac{\epsilon_C(\omega; \phi) - \epsilon_c(\omega)}{\epsilon_C(\omega; \phi) + 2\epsilon_c(\omega)} \lambda(\phi) \mu(\phi) d\phi + \int_0^1 \frac{\epsilon_B(\omega; \phi) - \epsilon_c(\omega)}{\epsilon_B(\omega; \phi) + 2\epsilon_c(\omega)} [1 - \lambda(\phi)] \mu(\phi) d\phi = 0, \tag{4}$$

where

$$\epsilon_C(\omega; \phi) = \epsilon_1(\omega) \left( 1 - \frac{1 - \phi}{[1 - \epsilon_2(\omega)/\epsilon_1(\omega)]^{-1} - \frac{1}{3}\phi} \right), \quad (5)$$

$$\epsilon_B(\omega; \phi) = \epsilon_2(\omega) \left( 1 - \frac{\phi}{[1 - \epsilon_1(\omega)/\epsilon_2(\omega)]^{-1} - \frac{1}{3}(1 - \phi)} \right). \quad (6)$$

Similarly to the classical mixing laws (1)–(3) the local porosity mixing law (4) does not contain free fit parameters because the local porosity distribution  $\mu(\phi)$  and the local percolation probabilities  $\lambda(\phi)$  are accessible to an independent measurement.

It should be noted that both  $\mu(\phi)$  and  $\lambda(\phi)$  are in general three-dimensional quantities. Measuring them from two-dimensional pore space images requires additional precautions for the interpretation of the results. Recently we have found [18] that in certain limiting cases the relationship between two-dimensional and three-dimensional local porosity distributions is given by a simple length scale rescaling transformation. Below we assume that such a rescaling of lengths is indeed justified at least in an approximate sense.

### 3. Waterfilled porous glass

The local porosity distribution  $\mu(\phi)$  has been measured from two-dimensional sections for the sintered glass bead system discussed in the introduction [16,5,6]. Thus far we have not been able to measure also the local percolation probabilities directly. Such measurements are required for a full test of local porosity theory. In the absence of such measurements different forms for  $\lambda(\phi)$  were employed to fit the calculated effective dielectric function to the measured experimental data. It was found that these fits do not depend sensitively on the detailed shape of  $\lambda$  but mainly on the value of the single parameter

$$p = \int_0^1 \mu(\phi) \lambda(\phi) d\phi, \quad (7)$$

which is the control parameter for the percolation transition underlying equation (4) and which gives the total fraction of percolating cells in the specimen. This is demonstrated in Fig. 2 where the experimental data of Fig. 1 are compared to the new mixing law (4) using the experimentally measured local porosity distribution. The measured effective dielectric function is represented as filled circles for the real part. The open circles give the conductivity calculated from the imaginary part. The left axis refers to the real part, while the right axis applies to the conductivity.

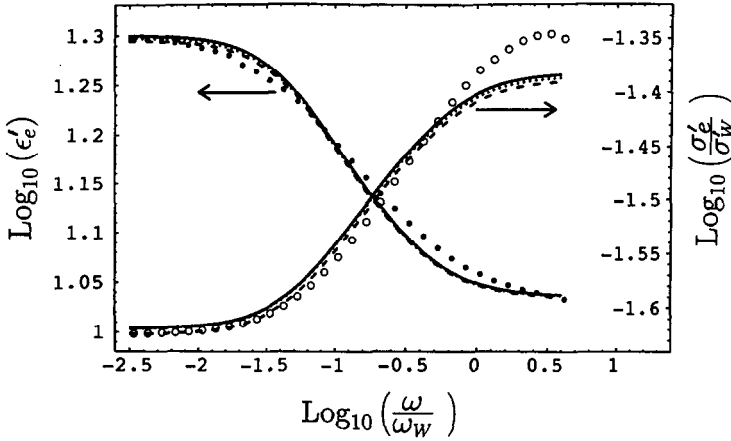


Fig. 2. Three fits of Eq. (4) to the same experimental data as in Fig. 1 with  $\lambda(\phi) = \phi^\gamma$  and  $\gamma = 0.2035$  for the solid line,  $\lambda(\phi) = \phi^{\gamma(1+C\phi)}$  with  $\gamma = 0.1524$  and  $C = 3.06$  for the dashed line, and a piecewise linear function  $\lambda(\phi)$  with breakpoint  $(\lambda_{b.p.} = 0.6155, \phi_{b.p.} = 0.0363)$  for the dotted line.

The lines in Fig. 2 represent theoretical fits for different forms of  $\lambda(\phi)$  involving one or two fit parameters. For the solid line we used the form  $\lambda(\phi) = \phi^\gamma$  and found  $\gamma = 0.2035$  as the best fit parameter. The dashed line assumes the form  $\lambda(\phi) = \phi^{\gamma(1+C\phi)}$  giving  $\gamma = 0.1524$  and  $C = 3.06$  as best fits. The dotted line is obtained by employing a piecewise linear form for  $\lambda$  with an adjustable breakpoint (b.p.) found as  $(\lambda_{b.p.} = 0.6155, \phi_{b.p.} = 0.0363)$ . In all cases  $\lambda(0) = 0$  and  $\lambda(1) = 1$ . It is seen that the fit does not depend on the functional form of  $\lambda$ . Calculating  $p$  from Eq. (7) on the other hand yields nearly identical values in all cases. Specifically, we find  $p = 0.594$  for the solid line,  $p = 0.589$  for the dashed line, and  $p = 0.607$  for the dotted line.

These findings suggest that the total fraction of percolating cells can be reliably determined by measuring the local porosity distribution and the effective dielectric function. In Fig. 3 we display the results of such measurements [5]. The results demonstrate that the sintering process is a  $p_c$ -approaching consolidation process in the sense of Ref. [8]. The horizontal line represents the percolation threshold value  $p_c = \frac{1}{3}$  within effective medium theory. If Archie's law holds for the sintering process then  $p(\bar{\phi})$  should remain above  $p_c$  as  $\bar{\phi} \rightarrow 0$ . Fitting a straight line through the data points fulfills this requirement. On the other hand we expect the presence of a percolation transition at a small but finite bulk porosity because of the generation of isolated pores from pockets formed by local tetrahedra of mutually touching glass beads. For this reason we have fitted a power law displayed as the straight line through the data points. We find  $p(\bar{\phi}) = 1.51 \times (\bar{\phi})^{0.45}$  as the best fit. This fit predicts a percolation threshold lower than  $\bar{\phi} \approx 0.035$  because the effective medium value for  $p_c$  overestimates the percolation threshold.

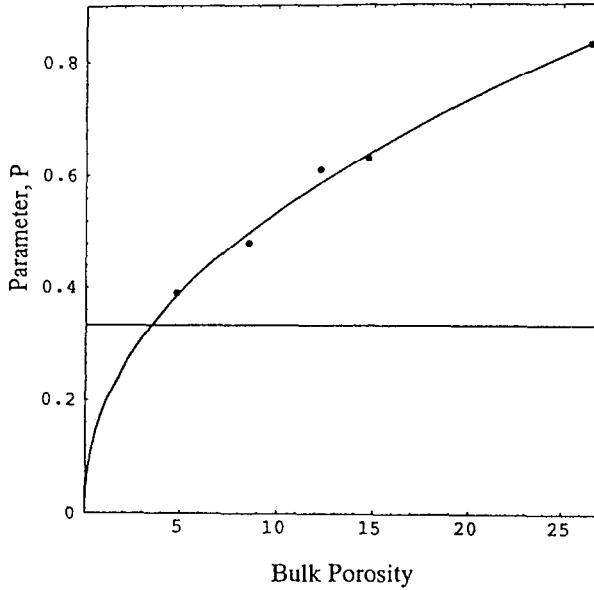


Fig. 3. Control parameter  $p$  (Eq. (7)) for the sintering of  $90\ \mu\text{m}$  glass beads as a function of bulk porosity  $\bar{\phi}$ .

#### 4. Polymer blends

In this section we show that the ideas underlying local porosity theory are not limited to dielectric dispersion arising from the Maxwell–Wagner effect. Recently Fischer and Zetsche [4,19] have suggested a concentration fluctuation model to explain the broadening of the dielectric  $\alpha$ -relaxation observed in polymer blends near the glass transition [20,13,12]. The purpose of this section is to show that their model may be viewed as a special case of local porosity theory. Moreover it is shown how information obtained from numerical simulations of polymer blends [2,3] can be incorporated into such calculations.

Mathematically the model of Fischer and Zetsche may be formulated as a simple non-selfconsistent average

$$\epsilon_e(\omega) = \int_0^1 \epsilon_{\text{loc}}(\omega, \phi) \mu(\phi) d\phi, \quad (8)$$

where  $\epsilon_{\text{loc}}(\omega, \phi)$  is an effective local dielectric function depending on the local volume fraction  $\phi$ . The linear extension  $L^*$  of the measurement cells is taken to be the size of “cooperatively rearranging units” near the glass transition. Fischer and Zetsche obtain the effective local dielectric function by interpolating all the parameters in the traditional Havriliak–Negami fit for the two pure polymers. The distribution of concentration fluctuations is assumed to be Gaussian. It is

then found that the width of this distribution increases with temperature for mixtures with an upper miscibility gap (LCST-behaviour).

The basic assumption of the concentration fluctuation model, Eq. (8), is reminiscent of Eq. (4). Setting  $\epsilon_C = \epsilon_{loc} = \epsilon_B$  in Eq. (4) yields a selfconsistent modification of the Fischer–Zetsche model as

$$\int_0^1 \frac{\epsilon_{loc}(\omega; \phi) - \epsilon_e(\omega)}{\epsilon_{loc}(\omega; \phi) + 2\epsilon_e(\omega)} \mu(\phi) d\phi = 0, \tag{9}$$

replacing Eq. (8). Note that the dependence on the connectivity of the microstructure within the “cooperatively rearranging domains” through  $\lambda(\phi)$  does not enter (9).

Instead of assuming a particular form for  $\mu(\phi)$  (in the absence of an experimental measurement) we propose to follow the original suggestion [7] and to extract  $\mu(\phi)$  from measurements of the order parameter distribution in a computer experiment. Such simulations have recently been carried out for the case of polymer mixtures [2,3]. The order parameter density  $P(m)$  of Fig. 2 in Ref. [2] is directly related to the local porosity distribution as  $P(m) = \mu(\phi/\phi_c - 1)$ , where  $\phi_c$  is the critical volume fraction for the unmixing transition.

As a third modification to the model of Fischer and Zetsche we use the simpler Debye form for  $\epsilon_{loc}$  instead of the Havriliak–Negami form. Thus we have [4,19]

$$\epsilon_{loc}(\omega, \phi) = \epsilon_\infty(\phi) + \frac{\epsilon_0(\phi) - \epsilon_\infty(\phi)}{1 + i\omega\tau(\phi)}, \tag{10}$$

with

$$\epsilon_0(\phi) = \phi\epsilon_{10} + (1 - \phi)\epsilon_{20}, \tag{11}$$

$$\epsilon_\infty(\phi) = \phi\epsilon_{1\infty} + (1 - \phi)\epsilon_{2\infty}, \tag{12}$$

for the interpolation of the relaxation strengths. The Vogel–Fulcher–Tammann law for the relaxation time

$$\tau(\phi) = A(\phi) \exp\left(-\frac{B(\phi)}{T - T_c(\phi)}\right) \tag{13}$$

is interpolated in the WLF-parametrization  $-\log(\tau/\tau_g) = c(\phi)[T - T_g(\phi)]/[d(\phi) + T - T_g(\phi)]$  through

$$A(\phi) = [\phi \log \tau_{g1} + (1 - \phi) \log \tau_{g2}] - [\phi c_1 + (1 - \phi)c_2], \tag{14}$$

$$B(\phi) = [\phi c_1 + (1 - \phi)c_2][\phi d_1 + (1 - \phi)d_2], \tag{15}$$

$$T_c(\phi) = [\phi T_{g1} + (1 - \phi)T_{g2}] - [\phi d_1 + (1 - \phi)d_2], \tag{16}$$

as suggested by Fischer and Zetsche. Here  $\tau_g$  is the  $\alpha$ -relaxation time at the calorimetric glass transition temperature  $T_g$  and the WLF-parameter  $d = T_g - T_c$  measures the width of the glass transition region.  $T_c$  is the Vogel–Fulcher–

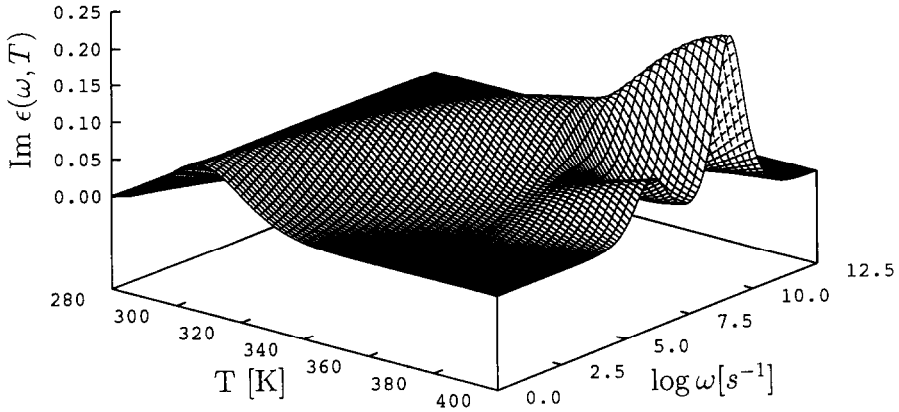


Fig. 4. Model calculation for the imaginary part of the dielectric function of a PVME/PS blend as function of temperature and frequency. The local porosity distribution was adapted from Ref. [2]. The total volume fraction is  $\bar{\phi} = 0.5$ . The values for the parameters of component 1 (PS) are:  $\epsilon_{10} = 2.8\epsilon_v$ ,  $\epsilon_{1\infty} = 3.0\epsilon_v$ ,  $\tau_g = 10^{-1.98}$  s,  $T_{g1} = 373.8$  K,  $c_1 = 9.33$ ,  $d_1 = 61.9$  K where  $\epsilon_v$  is the dielectric permittivity of vacuum. For component 2 (PVME) the values are:  $\epsilon_{20} = 3.2\epsilon_v$ ,  $\epsilon_{2\infty} = 2.0\epsilon_v$ ,  $\tau_g = 10^{-0.16}$  s,  $T_{g2} = 255.3$  K,  $c_2 = 13.66$  and  $d_2 = 61.6$  K.

Tammann temperature whose possible significance as an equilibrium phase transition temperature has recently become apparent [9]. The validity of the linear interpolation scheme has been confirmed experimentally in some cases [12].

In Fig. 4 we present solutions of Eq. (9) with a local porosity distribution  $\mu(\phi)$  adapted from Ref. [2] to an upper miscibility gap. The broadening of  $\mu(\phi)$  is consistent with that found by Fischer and Zetsche (cf. Fig. 4 of Ref. [4]). Fig. 4 shows a model calculation for the frequency and temperature dependent imaginary part of the dielectric function for a  $\bar{\phi} = 0.5$  mixture of Polyvinylmethylether (PVME) with Polystyrene (PS). The parameters for both substances are taken from [19] and reproduced in the figure caption. We have modelled the unmixing transition by adapting the order parameter distribution of Ref. [2] to the experimental situation with an assumed unmixing temperature around 370 K. Qualitatively the model calculation reproduces the observed features of the experiment.

### Acknowledgements

One of us (R.H.) is grateful to the Center for Advanced Study of the Norwegian Academy of Sciences for its hospitality, and to the Deutsche Forschungsgemeinschaft for partial financial support.

## References

- [1] F. Boger, J. Feder, T. Jøssang and R. Hilfer, Microstructural sensitivity of local porosity distributions, *Physica A* 187 (1992) 55.
- [2] H.P. Deutsch and K. Binder, Critical behaviour and crossover scaling in symmetric polymer mixtures: A Monte Carlo investigation, *Macromolecules* 25 (1992), 6214.
- [3] H.P. Deutsch and K. Binder, Simulation of first- and second-order transitions in asymmetric polymer mixtures, *Macromol. Chem. Macromol. Symp.* 65 (1993) 59.
- [4] E.W. Fischer and A. Zetsche, Molecular dynamics in polymer mixtures near the glass transition as measured by dielectric relaxation, *ACS Polymer Preprints* 33 (1992) 78.
- [5] B.D. Hansen, E. Haslund, R. Hilfer and B. Nøst, Dielectric dispersion measurements of salt-water saturated porous glass compared with local porosity theory, *Mat. Res. Soc. Proc.* 290 (1993) 185.
- [6] E. Haslund, B.D. Hansen, R. Hilfer and B. Nøst, Measurement of local porosities and dielectric dispersion for a water saturated porous medium, preprint (1993).
- [7] R. Hilfer, Geometric and dielectric characterization of porous media, *Phys. Rev. B* 44 (1991) 60.
- [8] R. Hilfer, Local porosity theory for flow in porous media, *Phys. Rev. B* 45 (1992) 7115.
- [9] R. Hilfer, Classification theory for nonequilibrium phase transitions, *Phys. Rev. E* 48 (1993) 2466.
- [10] R. Hilfer, Local porosity theory for electrical and hydrodynamical transport through porous media, *Physica A* 194 (1993) 406.
- [11] I. Holwech and B. Nøst, Dielectric dispersion measurements of salt-water saturated porous glass, *Phys. Rev. B* 38 (1989) 12845.
- [12] G. Katana, F. Kremer, E.W. Fischer and R. Plaetschke, Broadband dielectric study of binary blends of bisphenol-a and tetramethylbisphenol-a polycarbonate, *Macromol.* 26 (1993) 3075.
- [13] G. Katana, A. Zetsche, F. Kremer and E.W. Fischer, Dielectric  $\alpha$ -relaxation in polymer blends: Miscibility and fluctuations, *ACS Polymer Preprints* 33 (1992) 122.
- [14] J. Lafait and D.B. Tanner, eds., ETOPIIM 2, Proc. Second Internat. Conf. on Electrical Transport and Optical Properties of Inhomogeneous Media, *Physica A* 157 (1989).
- [15] R. Landauer, Electrical conductivity in inhomogeneous media, in: *Electrical Transport and Optical Properties of Inhomogeneous Media* (New York), J.C. Garland and D.B. Tanner, eds. (AIP, New York, 1978) p. 2.
- [16] B. Nøst, B.D. Hansen and E. Haslund, Dielectric dispersion of composite materials, *Phys. Scr.* T44 (1992) 67.
- [17] P.N. Sen, C. Scala and M.H. Cohen, A selfsimilar model for sedimentary rocks with application to the dielectric constant of fused glass beads, *Geophysics* 46 (1981) 718.
- [18] B. Virgin, R. Hilfer and E. Haslund, Scaling relations for local porosity distributions in two and three dimensions, preprint.
- [19] A. Zetsche, Dielektrische  $\alpha$ -Relaxation in binären Mischungen amorpher Polymere, Ph.D. thesis, Johannes-Gutenberg Universität Mainz (1992).
- [20] A. Zetsche, F. Kremer, W. Jung and H. Schulze, Dielectric study on the miscibility of binary polymer blends, *Polymer* 31 (1990) 1883.